Giant magnetocaloric effect in an exchange-frustrated $GdCrTiO_5$ antiferromagnet

M. Das, S. Roy, N. Khan, and P. Mandal
Saha Institute of Nuclear Physics, HBNI, 1/AF Bidhannagar, Calcutta 700064, India

(Received 10 April 2018; revised manuscript received 11 July 2018; published 17 September 2018)

We report the role of exchange frustration on the magnetocaloric properties of $GdCrTiO_5$. Due to the highly frustrated nature of magnetic interactions, in $GdCrTiO_5$, the long-range antiferromagnetic ordering of Gd^{3+} moments occurs at a much lower temperature $T_N = 0.9$ K and the magnetic cooling power enhances dramatically relative to that observed in several geometrically frustrated systems. Below 5 K, the isothermal magnetic entropy change $(-\Delta S_m)$ is found to be 36 J kg^{-1} K^{-1} for a field change (ΔH) of 7 T. $-\Delta S_m$ shows saturationlike behavior with decreasing T down to 2 K and is reversible in nature. The adiabatic temperature change ΔT_{ad} is 15.5 K for $\Delta H = 7$ T. These magnetocaloric parameters are significantly larger than that reported for several potential magnetic refrigerants, even for small and moderate field changes. The present result not only suggests that $GdCrTiO_5$ could be considered as a potential magnetic refrigerant at cryogenic temperatures but also promotes further studies on the role of exchange frustration on the magnetocaloric effect. In contrast, only the role of geometrical frustration on the magnetocaloric effect has been previously reported theoretically and experimentally investigated on very few systems.

DOI: 10.1103/PhysRevB.98.104420

I. INTRODUCTION

The potential technological applications of environment friendly magnetic refrigeration such as in space science, and liquefaction and storage of hydrogen in the fuel industry and to achieve subkelvin temperatures for basic research seek for the most efficient low-temperature magnetocaloric material [1–19]. Paramagnetic (PM) salts are the standard refrigerant materials to achieve the subkelvin temperature using adiabatic demagnetization technique. The high density and very large magnetic moments in a magnetic material enhance the efficiency of magnetic refrigeration [7–12,20]. Several rare-earth transition metal oxides and intermetallic compounds carrying large magnetic moments have become attractive candidates for the low-temperature magnetic refrigeration [21–30]. In these materials, the rare-earth magnetic moments order at low temperature and a strong suppression of the magnetic entropy takes place in the vicinity of the order-disorder phase transition with the application of magnetic field. However, the value of the magnetic entropy change ΔS_m decreases rapidly and becomes very small just few kelvin below the transition temperature and thereby limits the lowest temperature achievable by the magnetic refrigeration technique. This is one of the major drawbacks for refrigeration using magnetically ordered materials. Recently, it has been shown that magnetic frustration significantly enhances the cooling power due to the presence of finite residual magnetic entropy well below the Neel temperature [28–30]. Frustration leads to infinite degeneracy of the magnetic ground state, which implies the presence of a macroscopic number of local zero-energy modes in the absence of a magnetic field. However, in the presence of a magnetic field, a nondegenerate fully polarized spin state of the antiferromagnet is achieved above the saturation field. Adiabatic demagnetization of this state corresponds to condensation of the above-mentioned local zero-energy modes and thereby produces a large change in magnetic entropy. The role of frustration on the magnetocaloric effect has been investigated theoretically for classical Heisenberg antiferromagnets on different geometrically frustrated systems such as kagome, garnet, and pyrochlore lattices [31,32]. It has been observed that the pyrochlore lattice is the most frustrated among the above-mentioned three systems and offers the fastest cooling rate under adiabatic demagnetization [31,32]. The role of frustration, which is due to the bond dependent anisotropic exchange interactions or competing magnetic exchange interactions, on the magentocaloric effect should be explored for a complete understanding of the frustration induced enhancement of the magnetic cooling power.

The compounds of the type RMn_2O_5 (R being rare-earth ions), crystallizing in an orthorhombic structure (space group Pbam), have attracted a lot of attention due to their magnetoelectric coupling and magnetic-field induced ferroelectric behavior. Besides magnetoelectric properties, RMn_2O_5 shows the ability to be a good magnetic refrigerant at cryogenic temperatures [29,33–36]. However, little attention is given to the members of the family $RCrTiO_5$ isostructural to RMn_2O_5 [37–39]. In orthorhombic $RCrTiO_5$, the Cr^{3+} ions are interspaced between the R^{3+} and Ti^{4+} ions and the Cr^{3+} spins are collinear along the crystallographic c axis whereas the moments of R^{3+} lie on the ab plane [40,41]. The schematic crystal structure of $GdCrTiO_5$ is shown in Fig. 1 and the magnetic structure with the spin orientation of the magnetic sublattice has been shown in Fig. 2. In the present work, we have studied the magnetic and magnetocaloric properties of the $GdCrTiO_5$ compound. $GdCrTiO_5$ was chosen as a low-temperature refrigerant material for two main reasons: (i) the large spin momentum of localized $4f$ shell electrons of Gd^{3+} ($S = 7/2$) and (ii) the very low antiferromagnetic (AFM) transition temperature (T_N) of the Gd sublattice. The magnetic and thermodynamic properties suggest that $GdCrTiO_5$ is a

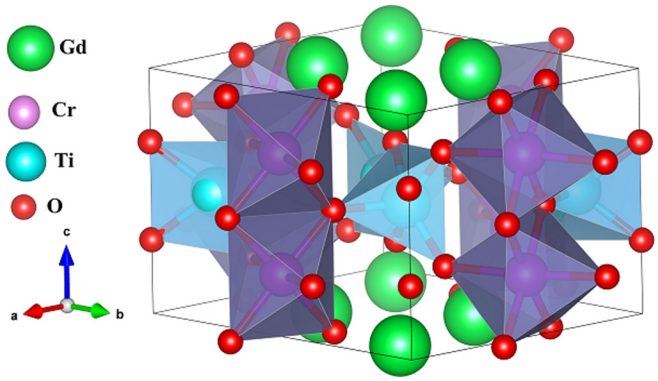

FIG. 1. The orthorombic crystal structure of $GdCrTiO_5$. The polyhedra formed by chromium (Cr) and titanium (Ti) with oxygen (O) atoms are shown schematically.

frustrated magnet [40–42]. Due to strong frustration, the Gd moments order at very low temperature (0.9 K), whereas the Cr^{3+} moments do not show any long-range ordering [40,42]. The competing magnetic exchange interactions from two sublattices are the origin of the frustration in the $GdCrTiO_5$ compound. To the best of our knowledge, there is no report on the large magnetocaloric effect for such type of exchange frustrated magnets. Also, $GdCrTiO_5$ is electrically insulating and the magnetization does not show thermal and field hysteresis, which are important criteria for magnetic refrigeration.

II. EXPERIMENTAL DETAILS

The polycrystalline $GdCrTiO_5$ sample was prepared by conventional solid-state reaction method using high purity Gd_2O_3 (99.9%), Cr_2O_3 (99.9%), and TiO_2 (99.9%) powders. Before use, Gd_2O_3 was pre-heated at 900 °C for 24 h. Well-mixed powders of Gd_2O_3, Cr_2O_3, and TiO_2 in a stoichiometric ratio 1:1:2 were heated at 1250 °C for few days with intermediate grindings. Finally, the green-colored $GdCrTiO_5$ sample was reground, pressed into pellets under high pressure and sintered at 1400 °C for 24 h in air followed by slow cooling. The phase purity and crystal structure of the sample

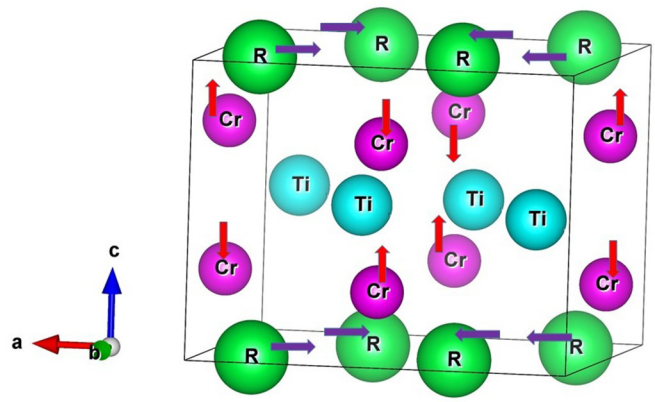

FIG. 2. Magnetic structure of $RCrTiO_5$ and the arrow indicates the orientation of magnetic moment of R^{3+} and Cr^{3+}. In $GdCrTiO_5$, the Gd moments order antiferromagnetically below 0.9 K but the Cr moments do not show any long-range ordering.

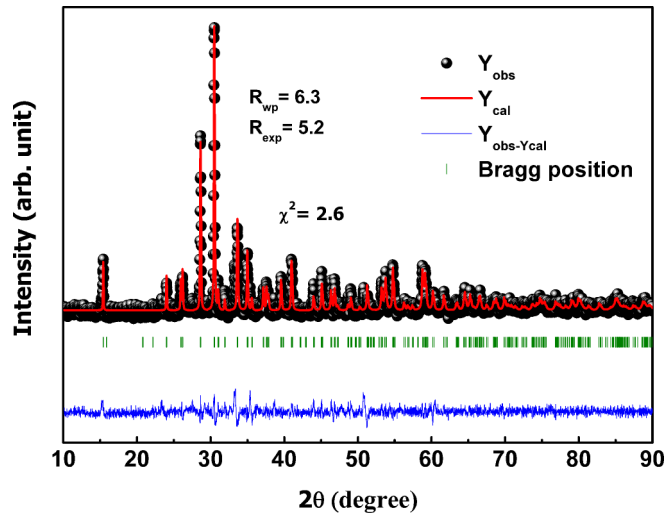

FIG. 3. The x-ray diffraction pattern of the polycrystalline powder of $GdCrTiO_5$ and the refinement parameters for the best fit result obtained from the profile fit are also shown.

have been determined by using high-resolution x-ray powder diffraction with CuK_α radiation (Rigaku TTRAX II) ($\lambda = 1.5406$ Å). The Rietveld refinement was used for the structural analysis of diffraction patterns of powdered $GdCrTiO_5$ sample with FULLPROF software. The experimental x-ray intensity profile along with the theoretical fit and the Bragg positions are shown in Fig. 3. All the observed peaks in the diffraction pattern can be indexed well with orthorhombic unit cell having Pbam crystallographic symmetry. Within the x-ray resolution, we did not observe any peak due to the impurity phase. The lattice parameters determined from the Rietveld profile analysis are $a = 7.4385$, $b = 8.5814$, and $c = 5.7782$ Å, which are very close to the reported values [42]. The atomic positions obtained from Rietveld refinement of room-temperature XRD of $GdCrTiO_5$ are presented in Table I. A small piece of rectangular shape sample was cut from the polycrystalline pellet for the magnetization (M) measurements. The temperature and magnetic field dependence of magnetization measurements have been carried out using a superconducting quantum interference device-vibrating sample magnetometer (SQUID-VSM, Quantum Design). For the isothermal magnetization, the data have been recorded in the field range 0–7 T at different temperatures between 2 and 35 K, and the temperature dependence of magnetization was

TABLE I. The atomic positions obtained from the Rietveld refinement of room-temperature XRD of $GdCrTiO_5$ compound.

Elements	X	Y	Z
Gd	0.16081	0.19045	0
Cr	0	0.5	0.15319
Ti	0.11930	−0.15443	0.5
O_1	0.11600	−0.27281	0.25618
O_2	0.15262	0.45428	0
O_3	0.15088	0.40262	0.5
O_4	0	0	0.3004

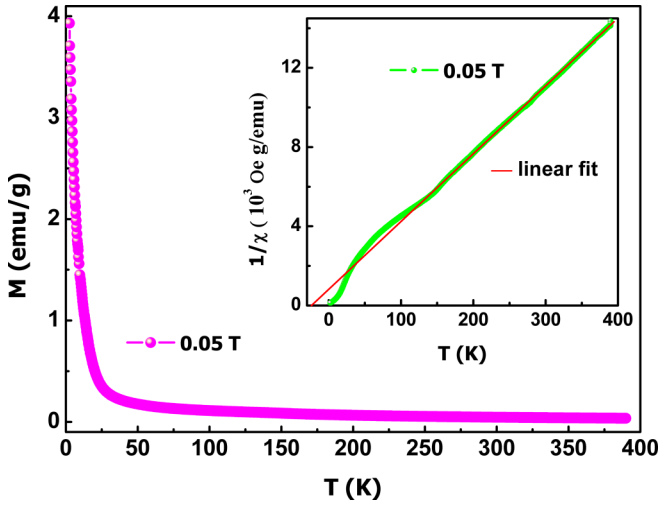

FIG. 4. The main panel shows the temperature dependence of magnetization for $GdCrTiO_5$ at 0.05 T and the inset shows the Curie-Weiss fit to inverse susceptibility (H/M) at high temperature.

measured in the range 1.8–400 K. The heat capacity (C_p) measurement was performed by relaxation method down to 1.8 K in applied fields up to 7 T in a physical property measurement system (PPMS, Quantum Design). The thermal conductivity was measured via a four-probe technique using the thermal transport measurement option in a physical property measurement system (Quantum Design). The typical dimension of the sample used in the thermal transport study is $4 \times 2 \times 1$ mm^3.

III. RESULTS AND DISCUSSION

The main panel of Fig. 4 shows the $M(T)$ curve of $GdCrTiO_5$ for an applied field of 500 Oe. M increases with decrease in T but no clear signature of long-range magnetic ordering is observed down to 2 K. For a better understanding of the nature of the magnetic ground state of $GdCrTiO_5$, the inverse dc susceptibility χ^{-1} ($\chi = M/H$) has been plotted as a function of temperature in the inset of Fig. 4. At high temperature above 150 K, the susceptibility follows the Curie-Weiss law, $\chi = C/(T - \theta_{CW})$, where C is the Curie constant and θ_{CW} is the Curie-Weiss temperature. From the linear fit to the high temperature data, we have calculated the values of the effective paramagnetic moment $\mu_{eff} = 8.8\ \mu_B$/f.u. and $\theta_{CW} = -24$ K. These values match well with the previously reported ones [41]. A negative θ_{CW} suggests that the dominating exchange interaction in $GdCrTiO_5$ is AFM. The above value of μ_{eff} is larger than the effective moment of Gd^{3+} (7.94 μ_B/Gd) ion in the PM state, indicating a contribution in susceptibility from both the Gd^{3+} ($S = 7/2$) and the Cr^{3+} ($S = 3/2$) spins.

With decreasing temperature, χ^{-1} starts to deviate from the linear behavior below ~150 K, which is quite high. This deviation of $\chi^{-1}(T)$ at high temperatures well above θ_{CW} may be due to the strong spin fluctuations in the PM state as a result of short-range magnetic correlations. Several frustrated rare-earth transition metal oxides exhibit strong spin fluctuations due to their nearly triangular network of the magnetic ions [43–46]. As a result, the long-range AFM ordering in these compounds sets-in at a much lower temperature than the deduced Curie-Weiss temperature; the magnetic energy scale of the system. The reduction of AFM transition temperature, T_N, is a signature of frustration and the value of the ratio θ_{CW}/T_N can be used as a measure of the spin frustration strength [43–45]. A spin system is classified as a strongly frustrated one if this ratio exceeds 10, because the simple mean-field theory fails to explain such a huge reduction in T_N [45]. In hexagonal manganites ($RMnO_3$), the maximum value of θ_{CW}/T_N is reported to be ~10 and these systems are considered to be strongly frustrated ones [43–45]. As the present system orders antiferromagnetically below 0.9 K and the observed values of θ_{CW} are within 24–33 K [41,42], we find $26 < \theta_{CW}/T_N < 37$, which is significantly larger than the value reported for the hexagonal manganites. Thus $GdCrTiO_5$ can be considered as a strongly spin frustrated system like several other multiferroics.

In $RCrTiO_5$ family of compounds, the detailed analysis of magnetic and thermodynamic properties has not been done so far. There are only few reports on magnetic and magnetoelectric properties of Nd-based compounds. Due to the presence of two sublattices, the magnetic properties of these materials are very complicated. For $NdCrTiO_5$, the temperature dependence of magnetization shows a very weak anomaly at 21 K and a sharp peak at 13 K. In earlier reports, the peak at 13 K was assigned to AFM transition of Cr^{3+} and Nd^{3+} moments [39]. However, the recent magnetic, magnetoelectric, and heat capacity data suggest that the Cr^{3+} moments undergo an AFM transition at 21 K and then induce the order of the Nd^{3+} moments via an exchange coupling, in contrast to a direct cooperative ordering of the Nd^{3+} spin subsystem [39]. On the contrary, in $GdCrTiO_5$, the significantly larger moment of Gd^{3+} as compared to Cr^{3+} causes a strong spin fluctuation and tries to suppress the ordering of Cr^{3+} sublattice. Only Gd moments show AFM ordering at very low temperature [42]. Basu *et al.* studied the dielectric response and Raman effect in this system as a function of temperature [40]. They observed a clear anomaly in both dielectric constant and loss factor above 100 K and this anomaly pronounces and shifts towards higher temperatures with the increase in frequency. Raman scattering also shows an anomaly below 150 K, where the inverse susceptibility curve starts to deviate from linearity. The observed phenomena have been attributed to short-range ordering of Cr^{3+} moments [40]. In $SmCrTiO_5$, the $M(T)$ curve shows a distinct feature at 180 K and downward curvature over a wide temperature range below 180 K, which is to some extent similar to that observed in $GdCrTiO_5$ and has been attributed to AFM ordering of Cr^{3+} moments [47]. The nature of phase transition is important in refrigeration technology. The second-order magnetic phase transition is always preferable than the first-order. Generally, second-order phase transition exhibits very low or no hysteresis, whereas the first-order transition may exhibit significant thermal and field hysteresis which is undesirable in magnetic cooling technology. The sharp λ-like anomaly at 0.9 K in the heat capacity of $GdCrTiO_5$ suggests a second-order nature of the AFM-PM transition [42]. In order to explore the influence of magnetic field on the magnetic ground state, we have measured the field dependence of the magnetization in $GdCrTiO_5$ up to 7 T at

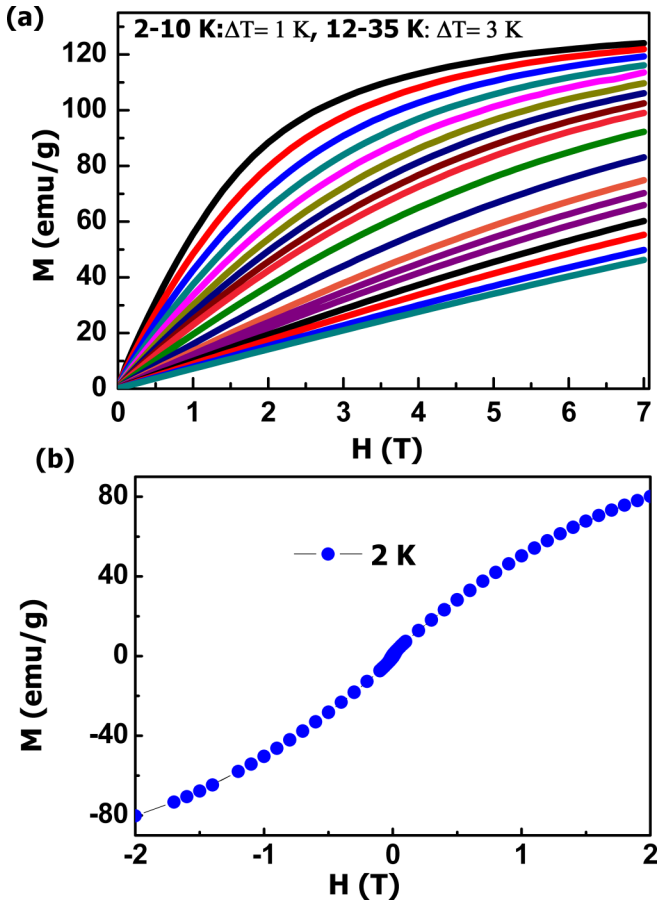

FIG. 5. (a) The isothermal magnetization plots for $GdCrTiO_5$ in the temperature range of 2–35 K and (b) the hysteresis loop at 2 K up to 2 T.

different temperatures in the range 2–35 K. The field dependence of M is shown in Fig. 5(a). M increases monotonically with the increase in H and tends to saturate at high fields and low temperature. $M(H)$ curves are like a Brillouin function of a paramagnet. At 2 K and 7 T, the value of the magnetic moment is 7.4 μ_B/f.u, which is about 6% higher than the spin only moment of Gd, indicating a small contribution from the Cr sublattice. We have measured the field dependence of M between −7 and 7 T at few temperatures. Figure 5(b) shows the five-segment $M(H)$ curve at 2 K for a field up to 2 T, as a representative. $M(H)$ does not display any hysteresis or anomaly. However, from the temperature dependence of the pyroelectric current measurement, it has been proposed that the strong alignment of the PM moments of Gd with an applied field $H > 1$ T forces a canting of Cr^{3+} moments for temperatures below 10 K and the canted moments of Cr^{3+} allow the inverse Dzyaloshinskii-Moriya interaction, which breaks the inversion symmetry of the crystal and gives rise to an improper spin-driven ferroelectric effect [41]. The absence of any anomaly in magnetization suggests that the effect of field-induced transition of Cr^{3+} moments on magnetic properties is very weak.

The field-induced isothermal magnetization indicates large magnetic entropy change in $GdCrTiO_5$. In order to test whether this material is suitable for magnetic refrigeration

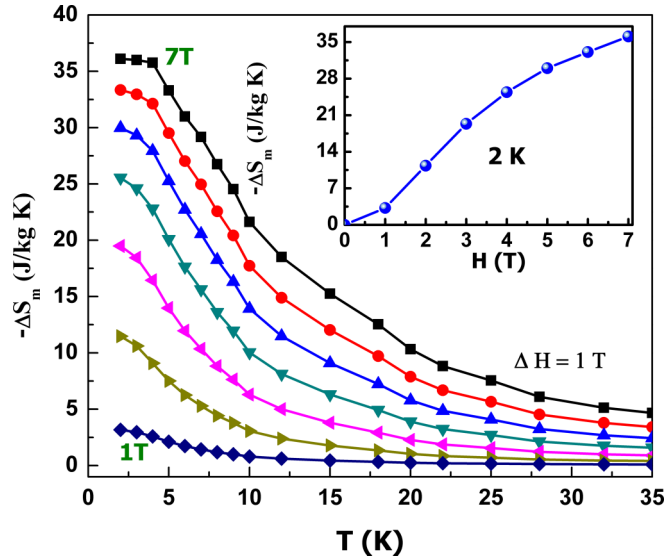

FIG. 6. The temperature variation of ΔS_m for $GdCrTiO_5$ calculated from the magnetization data and inset shows the field dependence of ΔS_m at 2 K.

in the low-temperature region, the magnetic entropy change has been calculated using the Maxwell equation, $\Delta S_m = \int_0^H (dM/dT)dH$. As the magnetization measurements are done at discrete field and temperature intervals, ΔS_m is numerically calculated using the following expression:

$$\Delta S_m = \sum_i \frac{M_{i+1} - M_i}{T_{i+1} - T_i} \Delta H_i, \quad (1)$$

where M_i and M_{i+1} are the magnetic moments at the temperatures T_i and T_{i+1}, respectively, for a change in magnetic field ΔH_i. Using the above equation, ΔS_m has been calculated from the magnetic field dependence of magnetization data at different temperatures. The temperature dependence of ΔS_m for field variation up to 7 T has been shown in Fig. 6. ΔS_m is found to be very large and negative down to the lowest measured temperature. The maximum value of ΔS_m $(-\Delta S_m^{max})$ increases with increase of the field and reaches as high as 36 J kg^{-1} K^{-1} for a field change of 0–7 T, which is more than double of the previously reported values of ΔS_m for other members of the RMn_2O_5 family [29,48,49]. We would also like to mention that the observed value of ΔS_m is significantly larger than that reported for several rare-earth transition metal oxides and intermetallic compounds [13–16]. A comparative study of ΔS_m of $GdCrTiO_5$ with other rare-earth based oxide compounds at same field and temperature range has been shown in Table II.

Apart from the value, the nature of temperature dependence of ΔS_m is very important for magnetic refrigeration. In a typical ferromagnet or antiferromagnet, ΔS_m increases with decreasing T in the PM state but it decreases rapidly below the onset of long-range ordering temperature, i.e., ΔS_m decreases on the both sides of T_C or T_N. In this context, it may be noted that undoped and doped $EuTiO_3$, $EuDy_2O_4$, and $GdVO_4$ exhibit huge magnetocaloric effect at low temperatures [50,51,53–55]. The values of ΔS_m^{max} in these compounds are also comparable to the present system. However, for

TABLE II. Comparison of magnetic entropy change (ΔS_m) and mechanical efficiency (η) of different magnetocaloric materials with respect to $GdCrTiO_5$

Materials	ΔH_0 (T)	ΔS_m (J kg^{-1} K^{-1})	η(%)	Ref.
$GdCrTiO_5$	2(5)	7.7(25.1)	51(37)	this work
$ErFeO_3$	2(5)	3(12)	47(19)	[25]
$TbCrO_3$	2(5)	4(12)	20(17)	[52]
$HoMnO_3$	2(5)	1(3)	19(18)	[28]
$DyMnO_3$	2(5)	0.2(3.8)	3(2)	[28]
$HoMn_2O_5$	2(5)	1(4)	15(7.4)	[29]
$GdVO_4$	2(5)	0.27(1.06)	44(40)	[51]
$EuDy_2O_4$	2(5)	8(20)	30(20)	[53]
$Er_2Mn_2O_7$	2(5)	1.25(2.24)	7(3)	[57]
Er_2MnTiO_7	2(5)	0.917(2.18)	5(2.9)	[58]

T_0(=5 K), operating temperature; ΔH_0, change in applied magnetic field; data for $\Delta H_0 = 5$ T are presented in the parentheses.

the compounds mentioned above, $\Delta S_m(T)$ shows a strong decrease in the low-temperature region and in some cases, ΔS_m may become small positive. On the other hand, ΔS_m in the present system does not decrease down to 2 K but a saturationlike behavior appears below 5 K for fields above 5 T. For application, ΔS_m should be reasonably large at the low or moderate magnetic field strength. The field dependence of ΔS_m is displayed in the inset of Fig. 6 at 2 K. From the contour plots of ΔS_m with a temperature and a magnetic field as shown in Fig. 7, one can see that ΔS_m in the low-temperature region is quite large at low field. For example, the values of $-\Delta S_m$ at 2 K are 12 and 20 J kg^{-1} K^{-1} for a field change of 2 and 3 T, respectively, which can be achieved using a permanent magnet. Another remarkable feature of the low-field $\Delta S_m(T)$ curve is that instead of saturation behavior at low temperature, ΔS_m increases with decrease in T ($d\Delta S_m/dT < 0$). So, ΔS_m can be significantly large even in the sub-kelvin region. The saturationlike behavior of ΔS_m down to 2 K is due to the very low AFM transition of $GdCrTiO_5$.

The large magnetocaloric effect in $GdCrTiO_5$ is associated with infinite numbers of degenerate frustrated magnetic

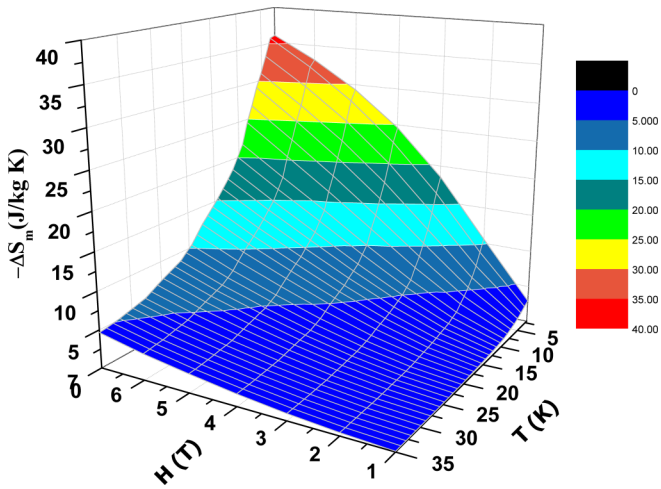

FIG. 7. The contour plot of ΔS_m as functions of temperature and magnetic field for $GdCrTiO_5$.

ground states. The frustration in the present compound occurs due to the competition between the Dzyaloshinskii-Moriya interaction and the spatial anisotropy exchange interaction, which is one of the main characteristics of RMn_2O_5 series. With application of magnetic field, the degeneracy in the ground state tends to lift and causes the frustrated magnetic moments to polarize in the field direction, as a result, large magnetic entropy change occurs. Theoretical investigations have shown that the enhancement of magnetocaloric effect in frustrated magnet is related to the condensation of soft modes below the saturation field [31]. However, there are very few experimental reports to support such theoretical prediction for large magnetocaloric effect in frustrated systems [30,32].

From the application perspective, the mechanical efficiency (η) is an important parameter for magnetic refrigeration, if the magnetocaloric effect is driven mechanically using a permanent magnet to generate a magnetic field. The heat (Q) is generated when a magnetic field is applied to an isothermal magnetocaloric material at the operating temperature T_0. As the direct calorimetric measurement is challenging, Q is calculated using the reported indirect method, i.e., from the temperature dependence of ΔS_m graph. The amount of mechanical work done (W) has been estimated by integrating $-MdB$ using the magnetization data. We have calculated $\eta = \|Q/W\|$ for $GdCrTiO_5$ and compared with different magnetocaloric materials, as shown in Table II [56]. From the Table II, one can see that the mechanical efficiency of $GdCrTiO_5$ is significantly larger as compared to several magnetic refrigerants in the same temperature and magnetic field range. We would like to mention that the mechanical efficiency of $GdCrTiO_5$ is about an order of magnitude larger than that for several geometrical frustrated systems such as $Er_2Mn_2O_7$ [57].

In order to understand the nature of magnetic ground state of $GdCrTiO_5$, we have measured the heat capacity. Figures 8(a) and 8(b) show the temperature dependence of heat capacity at different applied fields. At zero field, as shown in Fig. 8(a), initially C_p decreases with decreasing T down to 12 K and then increases with further decrease in T. No strong anomaly due to the long-range magnetic ordering has been observed within the measured temperature range of 1.8–300 K. However, a careful observation reveals an extremely weak anomaly at a temperature around 10 K, which is just above our experimental resolution. A similar weak anomaly in C_p has been reported earlier and attributed to short-range ordering [42]. The muon-spin rotation/relaxation study also shows an anomaly around 10 K [41]. The nature of the anomaly suggests that the transition is very weak and the entropy associated with this transition is negligible. The increase of C_p at low temperature indicates the onset of long-range ordering of Gd^{3+} sublattice below 1.8 K. With the application of a magnetic field, the nature of the low-temperature $C_p(T)$ curve changes drastically. Up to 2 T, C_p is enhanced with increase in field strength without showing any peak but a broad peak appears around 7 K at 5 T, which shifts further towards higher temperatures as the applied magnetic field is increased from 5 to 7 T.

The zero-field $C_p(T)$ curve can be fitted well with the combined Debye plus Einstein model over a wide temperature range as shown in Fig. 8(a). At low temperature, however,

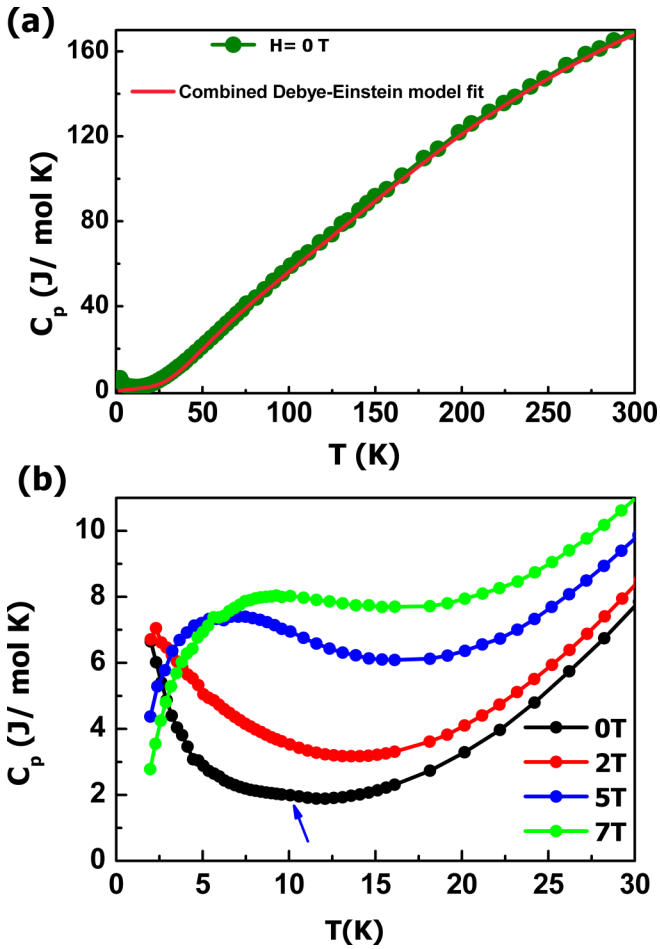

FIG. 8. (a) The zero-field heat capacity data for the $GdCrTiO_5$ compound and the solid line is the combined Debye-Einstein fit. (b) The field dependence of heat capacity for $GdCrTiO_5$. The arrow indicates the short-range ordering near 10 K.

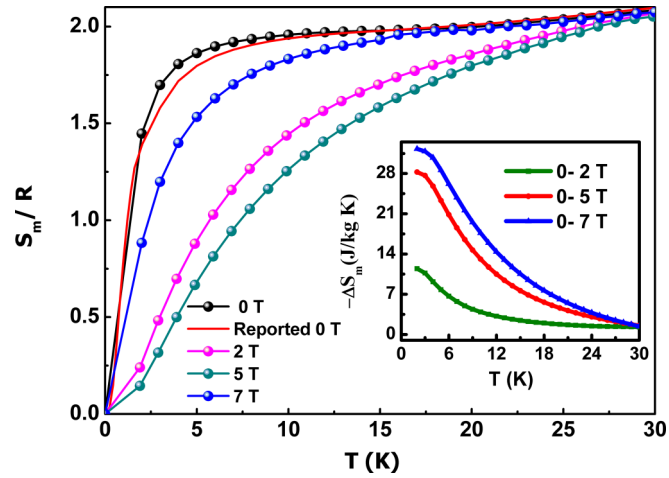

FIG. 9. The temperature variation of magnetic entropy with field for the $GdCrTiO_5$ compound, whereas the red line represents the zero field entropy calculated from reported data [42] and the inset shows the variation of ΔS_m calculated from the heat capacity data.

the fitted curve deviates from the observed experimental data. The lattice heat capacity calculated using the Debye plus Einstein model fitting was subtracted from the total heat capacity to determine the magnetic contribution (C_m). The magnetic entropy S_m is obtained by integrating $(C_m/T)dT$. As the AFM transition occurs well below 2 K, we can not determine the magnetic entropy using our heat capacity data for 0 and 2-T fields. However, this is not the case for the $C_p(T)$ curves at 5 and 7 T. For these fields, as the peak in $C_p(T)$ curve appears well above 2 K and the value of C_p is very small at low temperatures, the entropy change can be determined accurately by interpolating the $C_p(T)$ curves between 0 and 2 K using the methods described by others [59]. At high temperature, the entropy is expected to be close to the full saturated value $R\ln(2J+1) = 17.29$ J kg^{-1} K^{-1} for the Gd^{3+}. Figure 9 shows that S_m starts to saturate above 15 K and the saturated value is close to 17.2 J kg^{-1} K^{-1} for both $H = 5$ and 7 T. At high temperatures, well above T_N, the saturated value of entropy should nearly be the same for all fields even for the zero magnetic field. Comparing the deduced value of zero-field S_m above 1.8 K with that for 7-T field, we find that at zero field, a significant amount of entropy (10.7 J kg^{-1} K^{-1}) is released below 1.8 K. So, this extra amount was added to the zero-field entropy data to determine S_m for 0 T. For 2 T, the corresponding value is 7.7 J kg^{-1} K^{-1}. As the maximum normalized entropy (S_m)/R is very close to 2, we conclude that a major fraction of $4f$ spins of Gd^{3+} is taking part in the magnetic ordering. We have also calculated the zero-field magnetic entropy using the reported heat capacity data at low temperature (0.05–20 K) and observe that the deduced value of S_m is close to that obtained by interpolation, which is also shown in the main panel of Fig. 9 [42].

To check the consistency in our results on magnetic entropy change estimated from the $M(H)$ data, ΔS_m has also been calculated independently from the field dependence of heat capacity using the relation $\Delta S_m = \int_0^T [C_p(H_2, T) - C_p(H_1, T)]/T\,dT$, where $C_p(H, T)$ is the specific heat at a field H. ΔS_m as calculated from the heat capacity data is shown in the inset of Fig. 9 for different fields as a function of temperature. To calculate ΔS_m, we have used the reported low-temperature $C_p(T)$ data at zero field [42]. The calculated values of ΔS_m are very close to that estimated from our zero field $C_p(T)$ curve. It is clear from the plots that the values of ΔS_m estimated from the heat capacity data are close to that calculated from magnetization. For an example, the calculated value of ΔS_m^{max} from magnetization is 30 J kg^{-1} K^{-1}, whereas that from the heat capacity data is 28.4 J kg^{-1} K^{-1} for the same field change 0–5 T. The small difference in the value of ΔS_m^{max} may be due to the underestimation of the magnetic heat capacity.

Another very important parameter related to magnetic refrigeration is ΔT_{ad}, which is the isentropic temperature difference between $S(H, T)$ and $S(0, T)$. For this, we have calculated the entropy $S(H, T)$ at field H after subtracting $\Delta S_m(H, T)$, determined using the heat capacity data, from the zero-field entropy $S(0, T)$. The temperature variation of entropy at different fields has been shown in Fig. 10. Figure 11 shows the temperature dependence of ΔT_{ad}. The maximum value of ΔT_{ad} is as high as 15.5 K at 7 T. Thus both ΔS_m and ΔT_{ad} are large for $GdCrTiO_5$. Similar to ΔS_m, ΔT_{ad} is also quite large at low and moderate field strength. However, there

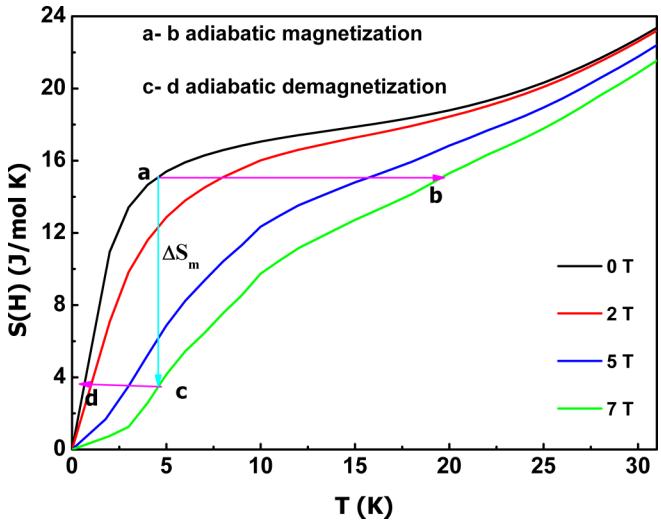

FIG. 10. The variation of entropy at different fields. The horizontal arrow from a to b indicates the adiabatic heating and c to d indicates the adiabatic cooling, whereas the vertical arrow indicates the isothermal entropy change for the magnetic field change 0–7 T.

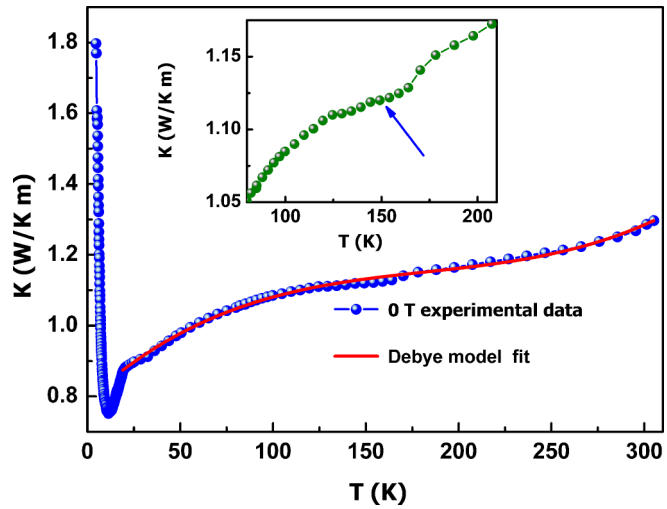

FIG. 12. The main panel shows the temperature dependence of thermal conductivity for $GdCrTiO_5$ whereas the red line shows the Debye fitting to the experimental data and the inset shows the anomaly near 150 K.

is an asymmetry in the $\Delta T_{ad}(T)$ curve at about 12 K, when applying a field adiabatically (ΔT_{ad} heating) and removing the field adiabatically (ΔT_{ad} cooling). The entropy increases rapidly in zero applied field but increases at a slower rate in the presence of a magnetic field. So, to interpret the deduced values of adiabatic temperature change, in Fig. 10, we have shown the actual heating (a to b arrow) and cooling (c to d arrow) effects due to adiabatic magnetization and adiabatic demagnetization, respectively. These two processes explain the difference between cooling and heating cycles in the magnetocaloric effect of $GdCrTiO_5$.

The cooling effect due to the adiabatic removal of magnetic field can be realized from the inset of Fig. 11. The final temperature (T_f) can be reached by an adiabatic demagnetization

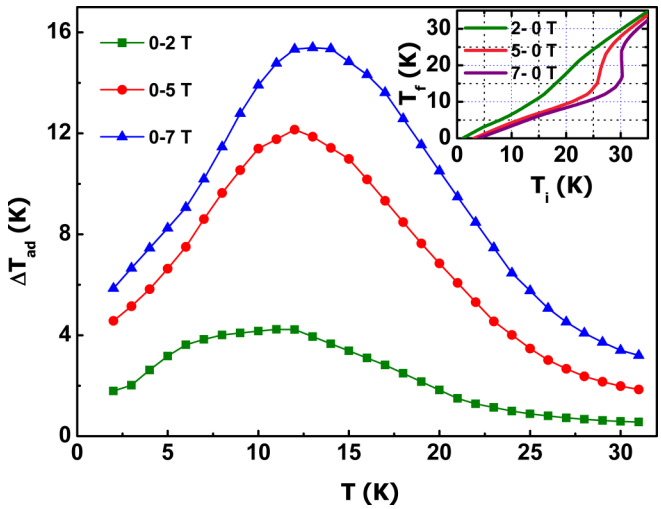

FIG. 11. The temperature dependence of ΔT_{ad} for $GdCrTiO_5$ at different magnetic fields and the inset shows the final temperature T_f as a function of the initial temperature T_i in the adiabatic demagnetization process for different magnetic fields.

from an initial temperature T_i, as presented pictorially in the inset of Fig. 11. For example, if the sample is initially at 30 K and magnetized by 7 T, decreasing the magnetic field adiabatically to zero causes the sample temperature to drop at 16 K. The lower the T_i, the lower is the T_f. Similarly, the adiabatic removal of magnetic field from 7 to 0 T at initial temperature $T_i = 20(5\text{ K})$ leads to $T_f = 8(0.12\text{ K})$.

For magnetic refrigeration, the used material should have reasonably high thermal conductivity (κ) for fast heat exchange and very high electrical resistivity to avoid any loss due to the eddy current. For this reason, we have measured the thermal conductivity of the studied material $GdCrTiO_5$ in the absence of a magnetic field. The main panel of Fig. 12 shows the temperature dependence of κ in the range 4–300 K. κ decreases very slowly with decrease in temperature down to 18 K and shows a deep around 11 K. Below 11 K, κ increases sharply and reaches as high as 1.8 W K^{-1} m^{-1} at 4 K. This behavior of κ is very similar to heat capacity and indicates a magnetic origin. The experimental data above 18 K can be fitted well with the Debye model. In several rare-earth transition metal oxides, κ starts to increase as temperature decreases and approaches towards the AFM transition of R^{3+} sublattice, where the phonon contribution becomes less important. The increase of κ with decrease in T at low temperature has been attributed to the suppression of spin-phonon scattering [60–65]. Besides phonons, magnons can also contribute to thermal conductivity at low temperature. From the inset of Fig. 12, it is clear that thermal conductivity shows a weak anomaly near 150 K where the magnetic susceptibility, and magnetodielectric and Raman scattering showed a change. Thermal conductivity measurements with magnetic field down to very low temperatures on single-crystalline samples will be useful for understanding the role of different scattering mechanisms. In the context of magnetocaloric effect, we would like to mention that the observed value of thermal conductivity of $GdCrTiO_5$ is comparable with that reported for several low-temperature magnetic refrigerants [65–67].

IV. SUMMARY

In summary, we have studied the magnetocaloric properties of $GdCrTiO_5$ through magnetization, heat capacity, and thermal conductivity measurements. In $GdCrTiO_5$, the magnetocaloric parameters are quite large. The maximum values of isothermal entropy change and adiabatic temperature change are 36 J kg^{-1} K^{-1} and 15.5 K, respectively, at 7 T. This compound also demonstrates a remarkable magnetocaloric effect even at low and intermediate applied fields. Unlike several potential low-temperature magnetic refrigerants, ΔS_m in the present compound does not decrease at low temperature and efficiency is very high due to the very low AFM transition of the Gd^{3+} sublattice. Our result suggests that $GdCrTiO_5$ could be a potential material for magnetic refrigeration at low temperature.

ACKNOWLEDGMENT

The authors would like to thank A. Pal for technical help during sample preparation and A. Pariari for the thermal conductivity measurements.

[1] K. A. Gschneidner, Jr., V. K. Pecharsky, and A. O. Tsokol, Rep. Prog. Phys. **68**, 1479 (2005).
[2] O. Gutfleisch, M. A. Willard, E. Bruck, C. H. Chen, S. G. Sankar, and J. P. Liu, Adv. Mater. **23**, 821 (2011).
[3] B. G. Shen, J. R. Sun, F. X. Hu, H. W. Zhang, and Z. H. Cheng, Adv. Mater. **21**, 4545 (2009).
[4] B. F. Yu, Q. Gao, B. Zhang, X. Z. Meng, and Z. Chen, Int. J. Refrig. **26**, 622 (2003).
[5] J. Liu, T. Gottschall, K. P. Skokov, J. D. Moore, and O. Gutfleisch, Nat. Mater. **11**, 620 (2012).
[6] O. Tegus, E. Bruck, K. H. J. Buschow, and F. R. De Boer, Nature (London) **415**, 150 (2002).
[7] M. Foldeaki, R. Chachine, and T. K. Bose, J. Appl. Phys. **77**, 3528 (1995).
[8] V. K. Pecharsky, and K. A. Gschneidner, Jr., Phys. Rev. Lett. **78**, 4494 (1997).
[9] V. K. Pecharsky, and K. A. Gschneidner, Jr., J. Magn. Magn. Mater. **167**, L179 (1997).
[10] H. Zeng, C. Kuang, and J. Zhang, Bull. Mater. Sci. **34**, 825 (2011).
[11] P. J. von Ranke, V. K. Pecharsky, and K. A. Gschneidner, Jr., Phys. Rev. B **58**, 12110 (1998).
[12] J. C. Patnino and N. A. De Oliveira, Intermetal. **64**, 59 (2015).
[13] L. Li, K. Nishimura, W. D. Hutchison, Z. Qian, D. Huo, and T. Namiki, Appl. Phys. Lett. **100**, 152403 (2012).
[14] A. Rostamnejadi, M. Venkatesan, P. Kameli, H. Salamati, and J. M. D. Coey, J. Magn. Magn. Mater. **323**, 2214 (2011).
[15] M. Baazaoui, M. Boudard, and S. Zemni, Mater. Lett. **65**, 2093 (2011).
[16] R. Mondal, R. Nirmala, J. A. Chelvane, and A. K. Nigam, J. Appl. Phys. **113**, 17A930 (2013).
[17] E. Bruck, O. Tegus, D. T. C. Thanh, and K. H. J. Buschow, J. Magn. Magn. Mater. **310**, 2793 (2007).
[18] H. Wada and Y. Tanabe, Appl. Phys. Lett. **79**, 3302 (2001).
[19] E. Bruck, M. Ilyn, A. M. Tishin, and O. Tegus, J. Magn. Magn. Mater. **290**, 8 (2005).
[20] P. Mukherjee and S. E. Dutton, Adv. Funct. Mater. **27**, 1701950 (2017).
[21] P. Sarkar, P. Mandal, and P. Choudhury, Appl. Phys. Lett. **92**, 182506 (2008).
[22] K. Y. Jiao, Z. X. Qun, G. Heng, M. Yue, and C. Z. Hua, Chin. Phys. B **24**, 037501 (2015).
[23] Y. J. Ke, X. Q. Zhang, Y. Ma, and Z. H. Cheng, Sci. Rep. **6**, 19775 (2016).
[24] Y. Cao, M. Xiang, W. Zhao, G. Wang, Z. Feng, B. Kang, A. Stroppa, J. Zhang, W. Ren, and S. Cao, J. Appl. Phys. **119**, 063904 (2016).
[25] R. Huang, S. Cao, W. Ren, S. Zhan, B. Kang, and J. Zhang, Appl. Phys. Lett. **103**, 162412 (2013).
[26] M. Shao, S. Cao, Y. Wang, S. Yuan, B. Kang, and J. Zhang, Solid State Commun. **152**, 947 (2012).
[27] E. K. G. Lorusso, J. W. Sharples, E. Palacios, O. Roubeau, E. K. Brechin, R. Sessoli, A. Rossin, F. Tuna, E. J. L. Mclnnes, D. Collison, and M. Evangelisti, Adv. Mater. **25**, 4653 (2013).
[28] A. Midya, S. N. Das, P. Mandal, S. Pandya, and V. Ganesan, Phys. Rev. B **84**, 235127 (2011).
[29] M. Balli, B. Roberge, P. Fournier, and S. Jandl, Crystals **7**, 44 (2017).
[30] S. Pakhira, C. Mazumdar, R. Ranganathan, S. Giri, and M. Avdeev, Phys. Rev. B **94**, 104414 (2016).
[31] M. E. Zhitomirsky, Phys. Rev. B **67**, 104421 (2003).
[32] S. S. Sosin, L. A. Prozorova, A. I. Smirnov, A. I. Golov, I. B. Berkutov, O. A. Petrenko, G. Balakrishnan, and M. E. Zhitomirsky, Phys. Rev. B **71**, 094413 (2005).
[33] G. R. Blake, L. C. Chapon, P. G. Radaelli, S. Park, N. Hur, S. W. Cheong, and J. Rodríguez-Carvajal, Phys. Rev. B **71**, 214402 (2005).
[34] Y. Ishii, S. Horio, M. Mitarashi, T. Sakakura, M. Fukunaga, Y. Noda, T. Honda, H. Nakao, Y. Murakami, and H. Kimura, Phys. Rev. B **93**, 064415 (2016).
[35] S. Wakimoto, H. Kimura, M. Feukunaga, K. Nishihata, M. Takeda, K. kakurai, Y. Noda, and Y. Tokura, Physica B **404**, 2513 (2009).
[36] J. M. Liu and S. Dong, J. Adv. Diel. **2**, 1530003 (2015).
[37] J. Saha, G. Sharma, and S. Patnaik, J. Magn. Magn. Mater. **360**, 34 (2014).
[38] M. Greenblatt, R. M. Hornreich, and B. Sharon, J. Solid State Chem. **10**, 371 (1974).
[39] J. Hwang, E. S. Choi, H. D. Zhou, J. Lu, and P. Schlottmann, Phys. Rev. B **85**, 024415 (2012).
[40] T. Basu, K. Sing, S. Gohil, S. Ghose, and E. V. Sampathkumaran, J. Appl. Phys. **118**, 234103 (2015).
[41] T. Basu, D. T. Adroja, F. Kolb, H.-A. Krug von Nidda, A. Ruff, M. Hemmida, A. D. Hillier, M. Telling, E. V. Sampathkumaran, A. Loidl, and S. Krohns, Phys. Rev. B **96**, 184431 (2017).
[42] E. B. Guedes, H. P. Martins, M. Abbate, S. H. Masuuaga, F. E. N. Ramirez, R. F. Jardim, and R. J. O. Mossanek, J. Alloys Compd. **724**, 67 (2017).

[43] T. J. Sato, S. H. Lee, T. Katsufuji, M. Masaki, S. Park, J. R. D. Copley, and H. Takagi, Phys. Rev. B **68**, 014432 (2003).
[44] T. Katsufuji, S. Mori, M. Masaki, Y. Moritomo, N. Yamamoto, and H. Takagi, Phys. Rev. B **64**, 104419 (2001).
[45] T. Katsufuji, M. Masaki, A. Machida, M. Moritomo, K. Kato, E. Nishibori, M. Takata, M. Sakata, K. Ohoyama, K. Kitazawa, and H. Takagi, Phys. Rev. B **66**, 134434 (2002).
[46] B. Paul, S. Chatterjee, A. Roy, A. Midya, P. Mandal, V. Grover, and A. K. Tyagi, Phys. Rev. B **95**, 054103 (2017).
[47] X. L. Qian, Y. F. Fang, J. Kang, S. X. Cao, and J. C. Zhang, Phys. B **495**, 1 (2016).
[48] M. Balli, S. Jandl, P. Fournier, and D. Z. Dimitrov, Appl. Phys. Lett. **108**, 102401 (2016).
[49] G. Heng, Z. X. Qun, K. Y. Jiao, J. J. Ling, L. Z. Xin, and C. Z. Hua, Chin. Phys. B **22**, 057502 (2013).
[50] A. Midya and P. Mandal, J. Appl. Phys. **116**, 223905 (2014).
[51] K. Dey, A. Indra, S. Majumdar, and S. Giri, J. Mater. Chem. C **5**, 1646 (2017).
[52] L. H. Yin, J. Yang, P. Tong, X. Luo, C. B. Park, K. W. Shin, W. H. Song, J. M. Dai, K. H. Kim, X. B. Zhu, and Y. P. Sun, J. Mater. Chem. C **4**, 11198 (2016).
[53] A. Midya, N. Khan, D. Bhoi, and P. Mandal, Appl. Phys. Lett. **101**, 132415 (2012).
[54] A. Midya, P. Mandal, K. Rubi, R. Chen, J. S. Wang, R. Mahendiran, G. Lorusso, and M. Evangelisti, Phys. Rev. B **93**, 094422 (2016).
[55] S. Roy, N. Khan, and P. Mandal, Appl. Mater. **4**, 026102 (2016).
[56] X. Moya, E. Defay, V. Heine, and N. D. Mathur, Nat. Phys. **11**, 202 (2015).
[57] N. B. Amor, M. Bejar, E. Dhahri, M. A. Valente, J. L. Garden, and E. K. Hlil, J. Alloys Compd. **563**, 28 (2013).
[58] N. B. Amor, M. Bejar, E. Dhahri, M. A. Valente, J. L. Garden, and E. K. Hlil, J. Sup. Nov. Magn. **26**, 3455 (2013).
[59] E. Palacios, J. A. Rodríguez-Velamazán, M. Evangelisti, G. J. McIntyre, G. Lorusso, D. Visser, L. J. deJongh, and L. A. Boatner, Phys. Rev. B **90**, 214423 (2014).
[60] S. Y. Li, L. Taillefer, C. H. Wang, and X. H. Chen, Phys. Rev. Lett. **95**, 156603 (2005).
[61] J. D. Song, C. Fan, Z. Y. Zhao, F. B. Zhang, J. Y. Zhao, X. G. Liu, X. Zhao, Y. J. Liu, J. F. Wang, and X. F. Sun, Phys. Rev. B **96**, 174425 (2017).
[62] J. D. Song, X. M. Wang, Z. Y. Zhao, J. C. Wu, J. Y. Zhao, X. G. Liu, X. Zhao, and X. F. Sun, Phys. Rev. B **95**, 224419 (2017).
[63] P. A. Sharma, J. S. Ahn, N. Hur, S. Park, S. B. Kim, S. Lee, J. G. Park, S. Guha, and S. W. Cheong, Phys. Rev. Lett. **93**, 177202 (2004).
[64] X. Zhao, J. C. Wu, Z. Y. Zhao, Z. Z. He, J. D. Song, J. Y. Zhao, X. G. Liu, X. F. Sun, and X. G. Li, Appl. Phys. Lett. **108**, 242405 (2016).
[65] X. M. Wang, C. Fan, Z. Y. Zhao, W. Tao, X. G. Liu, W. P. Ke, X. Zhao, and X. F. Sun, Phys. Rev. B **82**, 094405 (2010).
[66] Y. Yang, Q. C. Zhang, Y. Y. Pan, L. S. Long and L. S. Zheng, Chem. Commun. **51**, 7317 (2015).
[67] K. Berggold, J. Baier, D. Meier, J. A. Mydosh, T. Lorenz, J. Hemberger, A. Balbashov, N. Aliouane, and D. N. Argyriou, Phys. Rev. B **76**, 094418 (2007).